**Dalton Transactions**

# Tuning Different Kinds of Entangled Metal-organic Frameworks through Modifying the Spacer Group of Aliphatic Dicarboxylate Ligands and Reactant Ratio †

Jin-Xia Yang,[a] Ji-Quan Zhai,[ab] Xin Zhang,[a] Ye-Yan Qin,[a] Yuan-Gen Yao[a],*

Taking advantage of the conformational flexibility of the bpp ligand and aliphatic dicarboxylic acids, six interesting entangled coordination polymers, $\{[Cd(fum)(bpp)(H_2O)]\cdot(H_2O)\}_n$ (1), $\{[Cd(fum)(bpp)_2]\cdot(H_2O)_5\}_n$ (2), $\{[Cd_2(suc)_{1.5}(bpp)_2(NO_3)(H_2O)_2]\cdot6H_2O\}_n$ (3), $\{[Cd(suc)(bpp)_2]\cdot(H_2O)_{1.5}\}_n$ (4), $\{[Cd_2(glu)_2(bpp)_3]\cdot10H_2O\}_n$ (5), $\{Cd(adp)(bpp)(H_2O)\}_n$ (6) have been prepared and structurally characterized (bpp = 1,3-bi(4-pyridyl)propane, fum = fumaric, suc = succinate, glu = glutaric, adp = adipic). Compounds 1 and 2 are comprised of undulated 2D $4^4$-sql networks. In the structure of compound 1, two identical undulated layers are parallel interpenetrated to each other to give a 2D→2D interpenetrating framework. For 2, the dangling arms projected from 2D layers are intercalated into the neighboring sheets, producing a 2D→3D polythreading framework. Compound 3 shows a rare example of 2D self-penetrating framework with a (3,4)-connected $(4^2\cdot6^3\cdot8)(4^2\cdot6)$ topology. Compound 4 presents an unusual 2D self-threading network with a novel 4-connected $\{4^2\cdot6^3\cdot8\}$ topology. Compound 5 displays an 3D self-penetrating system based on a 2D→3D parallel polycatenation array. Compound 6 exhibits an unprecedented 3D self-penetrating structure having both 1D+1D→1D polycatenation and 3D+3D→3D interpenetration characteristics. A comparison of these six compounds demonstrates that both the different spacer length of the aliphatic dicarboxylates and reactant ratio appear to play a significant role in the assembly of entangled frameworks. In addition, thermal stabilities and photoluminescence properties of 1−6 have been examined in solid states at room temperature.

## Introduction

Despite a large number of coordination polymers (CPs) have been rationally assembled recently, the construction of entangled systems still is a longstanding fascination for chemists due to their intriguing aesthetic structures and promising applications as functional materials[1,2]. Entangled system, such as interpenetration, polycatenane, polyrotaxane, polythreading and polynotting (self-penetrating networks), is a major subject in the area of coordination polymer frameworks, which has been well discussed in several comprehensive reviews by Robson, Batten, Ciani and co-workers[3]. Among many types of entanglements, the most frequently encountered are the interpenetrating networks[4], in which two or more independent networks pass through each other either in parallel or inclined mode. Polythreading[5] is characterized by the existence of closed loops as well as of rod or string elements that can thread through the loops. Self-penetration[6], as an important phenomenon in the realm of entangled networks, is a single network having the peculiarity that the smallest topological rings are catenated by other shorter rings belonging to the same net. In contrast to the aforementioned types of entanglements, self-threading[7] is a new threading mode found in single nets, in which closed loops are threaded by components from the network itself.

To date, a variety of entangled coordination polymers with complicated structures have been synthesized and documented[8]. Of these syntheses, the most effective and representative synthetic approach for generating new entangled networks is the elaborate choice of the well-designed organic ligands[9]. The structural change of the organic ligand such as the angle, spacer, functional groups and relative position of the donor can control and vary the topology of the final structures. Therefore, utilizing similar or isomeric ligands to construct CPs has turned out to be an effective way to explore the impact of organic ligand on the formation of structures. In our previous report[10], we employed a rigid bidentate linear ligand fumaric acid to react with Zn(II) atoms in the presence of auxiliary N-donor ligands to obtain five entangled coordination polymers. The result suggests that the chemical nature of N-donor ligands play a significant role in tuning the entangled modes of coordination networks. Following this synthetic strategy, herein, we choose four kinds of similar aliphatic dicarboxylic acids (fumaric acid, succinate acid, glutaric acid, adipic acid) in combination with Cd(II) centers and flexible ligand 1,3-bis(4-pyridyl)propane (bpp) to investigate the influence of the configurations of dicarboxylic acids on the tuning of entangled networks. Furthermore, compared with rigid fumaric acid, the flexible bpp ligand possesses advantages in constructing entangled networks because it can exist in anti–anti (TT), anti–gauche (TG), and two different gauche–gauche (GG and GG') conformations[11] to meet the geometry requirements of metal

centers. Moreover, the influence of molar ratios on the self-assembly process is also investigated. As a result, we successfully isolated six new CPs with distinct entanglements, {[Cd(fum)(bpp)(H$_2$O)]·(H$_2$O)}$_n$ **(1)** with 2D→2D interpenetration, {[Cd(fum)(bpp)$_2$]·(H$_2$O)$_5$}$_n$ **(2)** with 2D→3D polythreading, {[Cd$_2$(suc)$_{1.5}$(bpp)$_2$(NO$_3$)(H$_2$O)$_2$]·6H$_2$O}$_n$ **(3)** with 2D self-penetrating, {[Cd(suc)(bpp)$_2$]·(H$_2$O)$_{1.5}$}$_n$ **(4)** with 2D self-threading, {[Cd$_2$(glu)$_2$(bpp)$_3$]·10H$_2$O}$_n$ **(5)** and {Cd(adp)(bpp)(H$_2$O)}$_n$ **(6)** with 3D self-penetrating. Their syntheses, crystal structures, topologies, thermal stabilities, and photoluminescence properties were reported in this paper.

## Experimental Section

### Materials and Instrumentation

All reagents were received as reagent grade and used without any further purification. Elemental analyses of C, H and N were determined by an EA1110 CHNS-0 CE elemental analyzer. Infrared spectra of solid samples were recorded on a Nicolet Magna 750 FT-IR spectrometer in the range of 400~4000 cm$^{-1}$. Thermogravimetric analyses (TGA) were carried out on a Netzsch STA 449C thermal analyzer from room temperature to 800 °C with a heating rate of 10 °C min$^{-1}$ under a nitrogen atmosphere. Powder-XRD measurements were performed on a Rigaku Dmax2500 X-ray diffractometer with Cu Kα radiation (λ = 1.54056 Å) with a step size of 0.05°.The fluorescence spectra were measured on an Edinburgh FLS920 TCSPC fluorescence spectrophotometer at room temperature.

### Synthesis of {[Cd(fum)(bpp)(H$_2$O)]·(H$_2$O)}$_n$ (1)

A mixture of Cd(NO$_3$)$_2$·4H$_2$O (0.123 g, 0.4 mmol), H$_2$fum (0.076 g, 0.4 mmol), bpp (0.079 g, 0.4 mmol), and NaHCO$_3$(0.034, 0.8 mmol) was dissolved in 10.0 mL of distilled water. The resulting mixture was stirred for 30 min and placed in a 23 mL Teflon-lined stainless vessel, which was sealed and heated at 100 ºC for 48 h. After being slowly cooled to the room temperature, colorless block crystals of 1 were isolated. Yield: 82 % based on Cd. Anal. calcd for C$_{17}$H$_{20}$Cd N$_2$O$_6$: C, 44.27; H, 4.34; N, 6.08 %. Found: C, 44.12; H, 4.78; N, 6.31%. IR (KBr pellet, cm$^{-1}$): 3336 (m), 2944 (w), 1614 (s), 1568 (s), 1552 (s), 1504 (m), 1429 (m), 1385 (s), 1224 (w), 1200 (w), 1070 (w), 1016 (w), 982 (w), 803 (m), 688 (m), 610 (w), 517 (w).

### Synthesis of {[Cd(fum)(bpp)$_2$]·(H$_2$O)$_5$}$_n$ (2)

The preparation of **2** was similar to that of **1** except that he molar ratio of reactants was changed to 1:1:2:1. Colorless prism crystals of **2** were collected in a 39 % yield based on Cd. Anal. calcd for C$_{30}$H$_{40}$Cd N$_4$O$_9$: C, 50.49; H, 5.61; N, 7.85 %. Found: C, 50.26; H, 5.98; N, 7.11 %. IR (KBr pellet, cm$^{-1}$): 3412 (m), 2939 (w), 1611 (s), 1570 (s), 1503 (w), 1425 (m), 1389 (s), 1223 (m), 1070 (w), 1015 (m), 984 (w), 804 (m), 694 (m), 609 (w), 575 (w), 511 (m).

### Synthesis of {[Cd$_2$(suc)$_{1.5}$(bpp)$_2$(NO$_3$)(H$_2$O)$_2$]·6H$_2$O}$_n$ (3)

The preparation of **3** was similar to that of **1** except that H$_2$fum was used instead of H$_2$suc. Colorless prism crystals of **3** were collected in a 39 % yield based on Cd. Anal. calcd for C$_{32}$H$_{49}$Cd$_2$N$_5$O$_{17}$ (1000.58): C, 38.38; H, 4.90; N, 6.70. Found:

C, 38.62; H, 4.76; N, 6.49. IR (KBr pellet, cm$^{-1}$): 3432 (m), 2943 (w), 1615 (s), 1566 (s), 1502 (w), 1427 (s), 1385 (s), 1298 (m), 1227 (m), 1188 (w), 1153 (w), 1069 (w), 1016 (m), 966 (w), 937 (w), 891 (m), 849 (m), 818 (m), 797 (w), 679 (w), 611 (w), 570 (w).

### Synthesis of {[Cd(suc)(bpp)$_2$]·(H$_2$O)$_{1.5}$}$_n$ (4)

The same synthetic method as that for **3** was used except that the molar ratio of reactants was changed to 1:1:2:1. Colorless block crystals of **4** were collected in a 63 % yield based on Cd. Anal. calcd for C$_{60}$H$_{64}$Cd$_2$N$_8$O$_{11}$: C, 55.21; H, 4.91; N, 8.59 %. Found: C, 55.37; H, 4.72; N, 8.43 %. IR (cm-1): 3430 (m), 2920 (w), 1611 (s), 1570 (s), 1425 (s), 1396 (m), 1298 (m), 1224 (m), 1069 (w), 1013 (m), 887 (w), 846 (w), 813 (m), 796 (w), 607 (w), 572 (w).

### Synthesis of {[Cd$_2$(glu)$_2$(bpp)$_3$]·10H$_2$O}$_n$ (5)

The reaction was carried out in a procedure similar to that for **1**, using H$_2$glu (0.053 g, 0.4 mmol) instead of H$_2$fum. Colorless prism crystals of **5** were obtained in 26 % yield based on Cd. Anal. Calcd for C$_{49}$H$_{74}$Cd$_2$N$_6$O$_{18}$ (1259.8): C, 46.67; H, 5.87; N, 6.67. Found: C, 46.92; H, 5.25; N, 6.36. IR (cm-1): 3413 (m), 2938 (w), 1612 (s), 1571 (s), 1502 (w), 1415 (s), 1307 (w), 1224 (m), 1152 (w), 1069 (w), 1015(m), 907 (w), 848 (w), 806 (m), 643 (w) 612 (w), 515 (w).

### Synthesis of {Cd(adp)(bpp)(H$_2$O)}$_n$ (6)

The reaction was carried out in a procedure similar to that for **1**, using H$_2$adp (0.058 g, 0.4 mmol) instead of H$_2$fum. Colorless prism crystals of **6** were obtained in 47 % yield based on Cd. Anal. Calcd for C$_{38}$H$_{48}$Cd$_2$N$_4$O$_{10}$ (945.62): C, 48.22; H, 5.08; N, 5.92. Found: C, 48.52; H, 4.65; N, 5.66. IR (cm-1): 3239 (m), 2946 (m), 1612 (s), 1568 (s), 1502 (m), 1449 (s), 1410 (s), 1363 (w), 1313 (m), 1296 (w), 1222 (w), 1175 (w), 1145 (w), 1070 (w), 1015 (m), 929 (w), 884 (w), 858 (w), 817 (m), 717 (w), 651 (w), 614 (w), 517 (m).

## X-ray Crystallography.

X-ray crystal structure determination Reflection data of the five compounds **2-6** were collected on an Oxford Xcalibur E diffractometer, and compound **1** was collected on a Rigaku MM-007/Saturn 70 with graphite monochromatic Mo−Kα radiation (λ = 0.71073 Å). Absorption corrections were applied with the program SADABS[12].All structures were solved by direct methods and refined by full-matrix least-squares methods on $F^2$ by using the SHELX-97 program[13]. All non-hydrogen atoms were refined anisotropically and the hydrogen atoms were introduced on calculated positions and refined by a riding mode. Crystallographic data and structure refinement parameters for compounds **1–6** are collated in Table 1. Selected bond lengths and angles are given in Table S1-S6. (ESI†).

## Results and discussion

### Syntheses

The six coordination polymers were all synthesized under hydrothermal conditions. As we known, hydrothermal

synthesis is a relatively complicated process and the final products can be affected by a variety of reaction variables (pH values, reaction time, solvents, template, and reactant ratio, etc). In order to investigate the influence of the ligand flexibility on the entangled coordination polymers, we chose four kinds of aliphatic dicarboxylic acids with different molecular backbones as secondary ligands incorporated into the Cd-bpp system. Meantime, the effects of reactant ratio on structural construction were also explored in this system. Inspired by our previous work[14], we firstly introduced the rigid linear ligand ($H_2$fum) into the Cd-bpp system in a molar ratio of 1 : 1 : 1, yielding crystal product of compound **1**. With change of Cd-bpp-fum ratio into 1 : 2 : 1 under uniform reaction conditions, a structurally different compound, **2**, was formed. Encouraged by the successful isolation of compound **1** and **2**, the four-carbon dicarboxylate ligand with flexible C–C σ bond ($H_2$suc) was selected instead of $H_2$fum. Similarly, when using different metal-ligand ratios, two structurally distinct compound **3** and **4** were obtained. The results indicate that reactant ratio plays an important role in the formation of coordination polymers. To further verify the influence of the ligand flexibility, the five-carbon and six-carbon aliphatic dicarboxylate ligands ($H_2$glu/$H_2$adp) were employed, and two new 3D complicated architectures, compound **5** and **6**, were isolated, respectively. However, while further adjusting the reactant ratio, we only obtained either the same compounds or unidentified white powder products. Therefore, our synthetic route is schematically depicted in Scheme 1. Based on the aforementioned observations, reaction conditions such as the ligand flexibility and reactant ratio exert a critical effect on the formation of entangled coordination polymers. Additionally, in order to study whether temperature impact the final structures, numerous parallel experiments have been repeated in the range of 80–120 °C, which shows that the effect of temperature in this system was small and the same structural compounds were obtained in this range.

**Crystal Structure of 1**
Crystallographic analysis reveals that compound **1** crystallizes in the monoclinic group $P2_1/c$ and features a 2-fold parallel interpenetrated 2D→2D network motif. As depicted in Figure 1a, the asymmetric unit contains one Cd(II) ion, one $fum^{2-}$ anion, one bpp ligand, one aqua ligand and one lattice water molecule. Each Cd(II) ion is hepta-coordinated and exhibits a pentagonal-bipyramidal geometry, with five oxygen atoms from two chelating carboxylate groups and one nitrogen atom of bpp ligand occupying the basal plane, one pyridyl nitrogen and one aqua donor at the apical sites. Two carboxylate group of one fum ligand both show a bisdentate chelating mode. Each $fum^{2-}$ ligand acts as bi-node and bridges two Cd(II) atoms with the Cd⋯Cd distance of 9.44 Å. Each bpp ligand shows the *TT* conformation. The dihedral angle between two pyridine ring planes is 82.1°. Each bpp acts as bidentate bridging ligand and joins two Cd(II) atoms with the Cd⋯Cd distance of 12.98 Å. Four Cd atoms are interlinked by two $fum^{2-}$ and two bpp ligands, thus affording a square grid with a large window of 12.98×9.44 Å$^2$, which are further connected together into a 2D puckered (4,4) net (Figure 1b). The large

square windows and the corrugation of the single sheets allow another identical network to interpenetrate the square windows in a parallel mode, thus giving a 2-fold (2D→2D) interpenetrating network (Figure 1c and 1d).

<void space for Figure 1>

**Crystal Structure of 2**
Single-crystal X-ray diffraction measurement reveals that compound **2** crystallizes in the triclinic system with *P*-1 space group. The asymmetric unit contains one Cd(II) atom, two half $fum^{2-}$ ligand, two bpp ligands and five lattice water molecules. As shown in Figure 2a, the Cd(II) cation adopts a distorted pentagonal bipyramidal geometry, coordinating to four carboxylic O atoms from two $fum^{2-}$ anions and three N atoms from three different bpp ligands. The Cd–O bond distances are in the range of 2.385(8)–2.462(9) Å and the Cd–N bond distances are in the range of 2.338(10)–2.369(12) Å. For convenience, the $fum^{2-}$ ligands containing O1 and O3 are designated fum-A and fum-B, and the bpp ligands containing N1 and N3 are designed bpp-A and bpp-B, respectively. All Cd(II) cations are connected through $fum^{2-}$ and bpp-A ligands to give a typical 2D square grid sheet, which contains two kinds of rectangle windows [$Cd_2$(fum-A)$_2$(bpp-A)$_2$] and [$Cd_2$(fum-B)$_2$(bpp-A)$_2$] with the dimensions of 9.31×12.02 Å and 9.29×12.02 Å, respectively. However, the one-end coordinated bpp-B ligands, grafted up and down each 2D network, resemble lateral arms protruding from the both sides of the 2D grid sheet alternately (Figure 2b). All the sheets are stacked in a parallel manner and arranged in a staggered fashion, and the distance between two adjacent sheets is approximately 8.02 Å. Each dangling bpp-B ligand is disposed in a mutual *anti* orientation with respect to the layer plane with an effective length of about 11.64 Å (from one Cd(II) center to the uncoordinated terminal nitrogen of bpp) which paves the way for the generation of mutual polythreading. As a result, the dangling lateral bpp-B ligands projected from both sides of the 2D layer are intercalated into the rectangle windows of the two adjacent layers above and below. Only the [$Cd_2$(fum-A)$_2$(bpp-A)$_2$] rectangular windows of each sheet are threaded by two dangling arms coming from two opposite directions (Figure 2c and 2d). Therefore, these entangled modes result in an interesting 2D→3D polypseudo-threading framework.

<void space for Figure 2>

**Crystal Structure of 3**
Single-crystal X-ray structural analysis reveals that compound **3** crystallizes in the monoclinic group $P2_1/n$ and exhibits a fascinating 2D self-penetrating network. As depicted in Figure 3a, the asymmetric unit of **3** contains two crystallographically independent Cd centers, one and a half of $suc^{2-}$ ligands (suc-A(O1-O3), suc-B(O5-O6)), two bpp ligands (bpp-A(N1-N2), bpp-B(N3-N4)), two coordinated water molecules, one nitrate ion and six lattice water molecules. The Cd1 atom locates in a distorted {$CdN_2O_5$} pentagonal bipyramidal coordination environment with oxygen donors from coordinated water molecule and bpp pyridine nitrogen donors in the axial position. The equatorial plane of each coordination sphere

contains two oxygen atoms from one suc²⁻ ligands, two oxygen donors from coordinated nitrate ion and one nitrogen atom from one bpp ligand. While the six-coordinated Cd2 atom adopts a distorted octahedral coordination geometry which bonds to three oxygen donors from two suc²⁻ ligands, two nitrogen donors from two different bpp ligands and one oxygen donors from coordinated water molecule. Each bpp-B ligand binds to the Cd2 atoms using *TG* conformation to form a 1D crankshaft shaped chain along the *b* axis. Neighboring 1D crankshaft shaped chains are interconnected by the suc-B molecules into a (6,3) undulated sheet (Figure 3b and 3c). Similarly, the bpp-A ligands exhibit *TG* conformation and coordinate the Cd1 atoms to generate infinite crankshaft shaped [Cd(bpp-A)]ₙ chains (Figure 4d). Significantly, these 1D [Cd(bpp-A)]ₙ chains are threaded through the 2D 6³ sheet to yield a (1D)ₙ + 2D →2D polythreading aggregation (Figure 3e and 3f). Furthermore, these 1D [Cd(bpp-A)]ₙ chains and 2D 6³ sheet are subsequently connected via the suc-A ligands to generate an unusual 2D self-penetrating network (Figure 3g and 3h).

So far, only a few examples of 2D self-penetrating networks have been obtained. Among these examples, most of the 2D self-penetrating structures are derived from co-parallel interpenetrating sheets[15] or the passage of the rod through the circuit in the 2D sheet[16]. However, the structure of **3** is composed by the 1D chains and a 2D layer which are entangled without increasing the dimensionality of the overall framework, and it represents an unique self-penetrating type. Topologically, if Cd1 and Cd2 cations are viewed as 3-connected and 4-connected nodes, respectively, and the suc²⁻ and bpp ligands are simplified to be linear connector, the structure of **3** can be described as a 2-nodal (3,4)-connected 2D network with the Schläfli notation of $(4^2·6^3·8)(4^2·6)$ (Figure 3h). According to electronic databaes EPINET, RCSR, and TOPOS TTD[17], it is a new topology. In addition, strong hydrogen bonds are observed among the adjacent 2D sheets. As depicted in Figure 4a, the coordinated O1w molecules form hydrogen-bonds with the carboxylate oxygen O1 atoms of suc²⁻ anions (O1w–H1wa⋯O1d = 2.754 Å; symmetry codes: d = −*x*, −*y*, −*z*), which extend the 2D sheets into a 3D supramolecular architecture (Figure 4b). From the topological view point, if the hydrogen bonds are taken into account, the Cd1 atoms can be considered as 4-connected nodes. Therefore, the whole 3D supramolecular architecture exhibits a uninodal 4-connected **sxa** network with the Schläfli symbol of $(4^2·6^3·8)$ (Figure 4c).

<void space for Figure 3>

<void space for Figure 4>

### Crystal Structure of 4

As shown as in Figure 5a, the asymmetric unit consists of one crystallographically independent Cd(II) atom, one suc²⁻ ligand, two bpp ligands (bpp-A(N1-N2), bpp-B(N3-N4)), and one and half water molecules. Each seven-coordinated Cd(II) atom sits in a distorted pentagonal bipyramidal geometry, which is defined by four oxygen atoms (O1, O2, O3a and O4a) of two suc²⁻ ligands and one nitrogen atoms (N1) from from one bpp ligand at the equatorial plane, and two nitrogen

atoms (N3 and N2a) from two different bpp ligands in the axial positions. The Cd(II) atoms are connected by the suc²⁻ ligands in chelating mode into [Cd(suc)] helical chains with a pitch of 11.22 Å along crystallographic *b* axis. And the adjacent opposite handed chains are arranged alternately and further extended into an achiral 2D layer via the bpp-A ligands which adopt *TG* conformation (Figure 5b). From the topological view point, each Cd atom can be assigned to four-connected nodes, the bpp ligands and suc²⁻ anions are taken as linkers, the 2D sheet can be simplified into a 4-connected network with the Schläfli symbol of $\{4^2·6^3·8\}$, representing a new 2D topological prototype[17] (Figure 5c). One outstanding feature of the structure of **4** is that there is one type of dangling bpp ligands (bpp-B) in *TT* conformation, located up and down each 2D sheet, inserts into the parallelgrammic voids of the 2D layer to produce an unusual 2D self-threading motif (Figure 5d and 5e). As far as we know, this kind of 2D self-threading structure is quite rare in coordination polymers, and only few examples have been reported which are all originated from the $4^4$-**sql** nets[18].

<void space for Figure 5>

### Crystal Structure of 5

When the longer aliphatic dicarboxylate glu²⁻ ligand was introduced in the Cd-bpp system, compound **5** was isolated. It crystallizes in the monoclinic *C*222₁ non-centro space group. There are one Cd(II) atom, two halves of two crystallographically distinct glu²⁻ ligands (glu-A(O1-O2), glu-B(O3-O4)), one and a half of bpp ligands (bpp-A(N1-N2), bpp-B(N3)) in the asymmetric unit of **5** as shown in Figure 6a. Each Cd(II) shows a distorted {CdN₃O₃} octahedral coordination environment, in which the equatorial plane contains O1, O2, O3 from two distinct glu²⁻ and N2a from one bpp ligand. The axial positions are occupied by two nitrogen atoms from two bpp ligands with an N1–Cd1–N3 angle of 177.17(19) Å. The Cd-O bond distances fall in the region 2.272-2.488 Å, and the Cd-N bond distances averaging 2.362 Å are in the normal range (Table 5). A distance of 2.744(5) Å between Cd1 and O4 indicates the existence of weak interaction between them.

The bpp-A molecules adopt *TT* conformation and coordinate the Cd(II) centers to afford infinite 1D chains. The chains span two directions in the *ab* plane and can be divided into two sets which are separated by about 7.842 Å. And the two sets of arrays are bound by bpp-B bridges in a *GG* conformation resulting in a 2D T-shaped bilayer structure (Figure 6b and 6c). In addition, the glu-A ligands act as the pillars to connect the Cd(II) atoms with the Cd⋯Cd separation of 8.581 Å which consolidate the 2D structure (Figure 6d and 6e). As is usually found, the large distances between the two planes result in large cavities within the network. In order to stabilize the network, each bilayer net interlocks with two adjacent bilayer nets into a 2D→3D parallel interpenetrating array (Figure 6f). These parallel interpenetrating bilayers are further connected by glu-B ligands as linkers to generate a 3D self-penetrating framework (Figure 6g). Topological analysis of compound **5** reveals that it is a 5-connected uninodal **htp** network with a point symbol

$\{4^2 \cdot 6^7 \cdot 8\}$ (Figure 6h).By carefully looking into this structure, we notice that five kinds of distinct helical chains coexist in the 3D network running along *a*, *b* and *c* direction with the pitch of 20.627, 13.667, 20.683 Å, respectively (Figure 7).

5                    <void space for Figure 6>

                     <void space for Figure 7>

**Crystal Structure of 6**
When glu$^{2-}$ is replaced with longer adp$^{2-}$ ligand, a particularly fascinating 3D self-penetrating structure of **6** has been
10 obtained. Single-crystal X-ray structural analysis reveals that the asymmetric unit of **6** contains two crystallographically independent Cd(II) atoms, four adp$^{2-}$ anions (adp-A(O1-O2), adp-B(O3-O4), adp-C(O5-O6), adp-D(O7-O8)), two bpp ligands (bpp-A(N1-N2), bpp-B(N3-N4)), two coordinated
15 water molecules (Figure 8). Both Cd(II) atoms possess a distorted $\{CdN_2O_5\}$ pentagonal bipyramidal coordination environment, with bpp pyridyl nitrogen donors in the axial positions. The equatorial plane of each coordination sphere contains two chelating carboxylate groups from two adp$^{2-}$
20 ligand, and an additional oxygen donor from coordinated water molecule.

The bpp-A molecules present *TG* coordination conformation and bpp-B molecules adopt *TT* coordination conformation, respectively. Two kinds of bpp ligands coordinate Cd(II)
25 atoms in an alternate manner to generate fascinating left- and right-handed helical chains with a pitch of 27.58 Å corresponding to the length of the *c* axis (Figure 9a). The neighboring Cd(II) atoms are separated by distances of 14.683 Å and 14.152 Å. The left- and right-handed helical chains are
30 associated together by the adp-A ligands to build a 1D ladder of $[Cd_2(bpp)_2(adp)]_n$ with the rectangular windows of 9.80×27.58 Å$^2$ (Figure 9b and 9c). The presence of the large windows paves the way for the onset of intertwinement. As shown in Figure 10a and 10b, two sets of ladder chains are
35 interlaced to give rise to an interesting 1D+1D→1D interpenetrating network, exhibiting a clearly defined polycatenation arrangement. Meanwhile, the adp-B ligands connect two sets of interpenetrating ladders together into a 1D unique self-penetrating chain (Figure 10c and 10d). So far,
40 although a large number of 2D or 3D self-penetrating structures have been documented, the 1D self-penetrating chains are still rare. Furthermore, these self-penetrating chains are combined by the adp-D ligands to form a 3D open framework with 1-D channels running along the *c* axis (Figure
45 10e and 10f). As anticipated, in order to minimize the big void cavities and stabilize the framework, the potential voids formed by a single 3D network show incorporation of another identical network, thus giving a 2-fold 3D+3D→3D interpenetrating network (Figure 11a and 11b). Finally, the
50 interpenetrating 3D networks are further interconnected by adp-C ligands, resulting in an unusual self-penetrating framework (Figure 11c and 11d). As shown above, the unprecedented structure of **6** contains two distinct levels of self-penetration derived from 1D+1D→1D polycatenation and
55 3D+3D→3D interpenetration. To date, although many exotic self-penetrating structures are being documented each year, the coexistence of different entangled motifs, especially the

simultaneous occurrence of two levels of self-penetration in the same crystal structure is extremely rare.

60 A better insight into the nature of the involved framework can be achieved by the application of a topological approach. To illustrate the unique structure of **6**, each Cd(II) center, being connected by two adp$^{2-}$ and two bpp ligands, can be simplified as a 4-connected node, and the adp$^{2-}$ and bpp
65 ligands can be simplified into a linear linker. Accordingly, the whole network can be extended to a 4-connected **sxa** net with a point symbol of $6^6$.

                     <void space for Figure 8>

                     <void space for Figure 9>

70                   <void space for Figure 10>

                     <void space for Figure 11>

**Structural comparison and the factors influencing the network**
According to the comparison of the synthetic method and the
75 structures of compounds **1-6**, it is clear that the spacer length and flexibility of auxiliary ligands and the reactant molar ratio play important roles in the formation of the entangled coordination polymers.

On the one hand, we introduced four different aliphatic
80 dicarboxylate ligands (H$_2$fum, H$_2$suc, H$_2$glu, H$_2$adp) into the Cd-bpp system, aiming at exploring the influence of aliphatic dicarboxylate on the assembly and structure of MOFs. The geometrical parameters of aliphatic dicaboxylate ligands in compound **1–6** are listed in Table 2. Analyzing the structural
85 descriptions above, compounds **1**, **3**, **5**, and **6** are obtained from the same metal center and neutral ligand (bpp) under uniform reaction condition, and all dicarboxylate ligands are linear linkers, which differ in the spacer length and flexibility of aliphatic dicarboxylate ligands. The spacer groups of the
90 aforementioned aliphatic dicarboxylate ligands are –CHCH–, –(CH$_2$)$_2$–, –(CH$_2$)$_3$–, –(CH$_2$)$_4$–, respectively. Different spacer groups of dicarboxylate ligands can change the length of the ligand through various extents, which in turn varies the separation between the metal atoms. As shown in Table 2, in
95 compound **1**, rigid linear fum$^{2-}$ ligands link Cd(II) atoms with the Cd⋯Cd separation of 9.44 Å. When the π-bond (–CHCH–) spacer is replaced by flexible σ-bond (–CH$_2$CH$_2$–) spacer, the suc$^{2-}$ ligands in compound **3** display two kinds of conformations and bridge the Cd(II) atoms with Cd⋯Cd
100 separation of 7.05 and 9.50 Å. Obviously, as the same four carbon aliphatic dicarboxylate ligands, suc$^{2-}$ ligand is flexible than fum$^{2-}$ ligand. As a result, compound **3** features a complicated 2D self-penetrating network, whereas compound **1** exhibits a 2D→2D interpenetrating framework comprised of
105 simple 2D $4^4$-**sql** structures. When extending the spacer length into –(CH$_2$)$_3$–, the more flexible glu$^{2-}$ ligand bind the Cd(II) atoms with the Cd⋯Cd separation of 7.52 and 8.58 Å. The changeable backbone of glu$^{2-}$ is in favor of the occurrence of the helix. Consequently, five kinds of distinct helical chains
110 coexist in the 3D self-penetrating network, which induce the chirality of compound **5**. Compared with glu$^{2-}$ ligand, the adp$^{2-}$ ligand has an additional –CH$_2$– group. In compound **6**, adp$^{2-}$ ligands exhibit four types of conformations with the the

Cd⋯Cd separation of 7.52, 7.64, 9.80, and 10.54, respectively. The intricate conformations result in unprecedented self-penetrating framework derived from two-level hierarchical entanglement. As we know, in the dual ligand system, the conformational changes in one of the ligands are strongly affected by the other ligand. By changing the spacer length of dicarboxylate ligands, the dipyridyl ligands (bpp) present different conformations and dihedral angles between the pyridyl rings, which in turn affect the formation of the final structure (Table 2). From the above discussion, compounds **1**, **3**, **5**, and **6** represent a classical example in which the spacer length and flexibility of auxiliary ligands show significant effects on modulating the formation of metal−organic frameworks with various types of entanglements.

On the other hand, a comparison of two reactant systems (Cd-bpp-fum, Cd-bpp-suc) demonstrates that the reactant molar ratio remarkably affects the resulting structures. Each system is prepared by the same metal centers and identical linkers under uniform hydrothermal procedure except using different reactant ratio. For Cd-bpp-fum system, when the metal-ligand ratios are changed from 1 : 1 : 1 to 1 : 2 : 1, two different entangled frameworks ranging from 2-fold 2D→2D interpenetrating sheet (**1**) to 2D→3D polypseudo-threading framework (**2**) are obtained. The structural difference caused by reactant ratio also can be supported by compounds **3** and **4**. Compound **3** was obtained in Cd-bpp-suc molar ratio of 1 : 1 : 1, which features a complicated 2D self-penetrating framework consisting of $(1D)_n$ + 2D →2D polythreading aggregation. With change of Cd-bpp-suc ratio into 1 : 2 : 1, an unusual 2D self-threading motif, **4**, was isolated. Clearly, the different reactant ratios led to the structural discrepancy.

## Powder X-ray diffraction and thermal properties

The powder X-ray diffraction patterns for compounds **1**−**6** are presented in Figure S1 (Supporting Information). The diffraction peaks of both simulated and experimental patterns are in agreement with each other, demonstrating the phase purities of **1**−**6**. The difference in intensity of some diffraction peaks may be due to the preferred orientation of the crystalline powder samples.

Thermogravimetric (TG) experiments were performed on compounds **1-6** in the temperature range of 30−800 °C (Figure S2 in the Supporting Information). For compound **1**, a gradual weight loss in the range of 90 to 150 °C is attributed to the release of coordinated water molecules and lattice water molecules (obsd 7.51%, calcd, 7.81%). Decomposition of the anhydrous residue was observed at 245°C and end above 320 °C. The weight loss corresponds to the loss of bpp ligands (obsd 43.23%, calcd 42.97%). Upon further heating, the coordinated ligands were lost until the residue was CdO (obsd 26.84%, calcd 27.88%). The TG curve of compound **2** reveals a steady weight loss between room temperature and 100 °C corresponding to the departure of lattice water molecules (obsd 12.46%, calcd 12.62%), and then a plateau region follows until 160 °C. The further weight losses represent the decomposition of the framework. A total loss of 11.17 % is observed for **3** in the temperature range of 30−120 °C, which can be attributed to the loss of lattice water molecules (calcd

10.78 %), and the anhydrous compound begins to decompose at 230 °C forming an unidentified product. Compound **4** first losses the lattice water in 30−100 °C region (obsd 4.53%, calcd 4.14%), and the second step in the temperature range of 200–300 °C corresponds to the loss of the bpp ligand (obsd 57.88%, calcd 60.74%). The remaining weight of 18.61% is consistent with a deposition of CdO (calcd 19.69%). For **5**, the loss of uncoordinated water molecules (obsd 13.72 %, calcd 14.29%) is observed before 75 °C. The abrupt weight loss corresponding to the release of organic ligands starts at 150 °C and leads to the formation of CdO as the residue (obsd 21.15%, calcd 20.39%). For **6**, the mass remained largely stable until 90 °C, at which point a series of mass losses ensued. The weight loss of coordinated water molecules took place in the range 90−140 °C (obsd 3.56%, calcd 3.81%), and the anhydrous component began to decompose at 210 °C.

## Photoluminescence Properties

Recently, coordination polymers based on $d^{10}$ transition metal ions have received more and more attention owing to their interesting luminescent properties. Therefore, the luminescent properties of these six compounds were investigated at room temperature in the solid state. As shown in Figure 12, upon excitation of 360 nm, these six Cd(II) compounds are luminescent with the emission bands at 458 nm for **1**, 437 and 506 nm for **2**, 430 nm for **3** and **4**, 416 nm for **5**, and 408 nm for **6**, respectively. In order to understand the nature of these emission bands for these six Cd(II) compounds, the luminescent properties of the free aliphatic dicarboxylate and bpp ligands were also studied at the same conditions. Notably, the aliphatic dicarboxylate ligands are non fluorescent in the visible light range, and the bpp ligand is luminescent with the maxima emission at 468 nm ($\lambda_{ex}$=360 nm). According to the literature, the Cd(II) ion is difficult to oxidize or reduce because of the $d^{10}$ configuration. As a result, the luminescent emission bands of **1**, **3**, **4**, **5** and **6** can be tentatively assigned to intraligand charge transfer, the lower energy emission band (437 nm) of **2** can be assigned to intraligand charge transfer and the higher energy emission band (506 nm) of **2** can be assigned to ligand-to-metal charge transfer, as reported for other Cd(II) coordination polymers constructed from mixed N-donor and O-donor ligands[19]

<void space for Figure 12>

## Conclusions

Six new entangled MOFs with interesting architectures have been successfully synthesized by introduction of different aliphatic dicarboxylates into Cd-bpp systerm. These compounds display various entangled structural motifs, including 2D→2D interpenetrating sheet (**1**), 2D→3D polythreading array (**2**), 2D self-penetrating net (**3**), 2D self-threading net (**4**), and 3D self-penetrating net (**5**, **6**). The structural differences of the compounds demonstrate that the variations of the spacer length and flexibility of auxiliary ligands and reactant ratio are critical to the assemblies of MOFs in some particular systems. Additionally, the bpp ligands exhibit versatile conformation, which will be

responsible for structural diversity of the resulting coordination polymers. Thus, the present work not only show an aesthetic diversity of coordinative network chemistry, but can also represent a nice example of constructing functional MOFs by rational choice of organic ligands with specific functional groups and geometry.

## Acknowledgements

## Notes and references

$^a$ *Key Laboratory of Coal to Ethylene Glycol and Its Related Technology, Fujian Institute of Research on the Structure of Matter, Chinese Academy of Sciences, Fuzhou 350002 (P. R. China). E-mail: yyg@fjirsm.ac.cn.*
$^b$ *College of Chemistry, Fuzhou University, Fuzhou, Fujian 350116 (P. R. China).*

† Electronic Supplementary Information (ESI) available. CCDC reference numbers 1062162-1062167 [details of any supplementary information available should be included here]. See DOI: 10.1039/b000000x/

(1) (a) Blake, A.; Champness, N.; Hubberstey, P.; Li, W.; Withersby, M.; Schröder, M. *Coord. Chem. Rev.*, **1999**, *183*, 117. (b) Batten, S. R.; Hoskins, B. F.; Robson, R. *Chem.–Eur. J.*, **2000**, *6*, 156. (c) Eddaoudi, M.; Li, H.; Yaghi, O. M. *J. Am. Chem. Soc.*, **2000**, *122*, 1391. (d) Bu, X. H.; Tong, M. L.; Chang, H.C.; Kitagawa, S.; Batten, S. R. *Angew. Chem., Int. Ed.*, **2004**, *43*, 192. (e) Perry, J. J.; Kravtsov, V. C.; McManus, G. J.; Zaworotko, M. J. *J. Am. Chem. Soc.*, **2007**, *129*, 10076. (f) Kuang, X. F.; Wu, X. Y.; Yu, R. M.; Donahue, J. P.; Huang, J. S.; Lu, C. Z. *Nat. Chem.*, **2010**, *2*, 461. (g) Forgan, R. S.; Sauvage, J. P.; Stoddart, J. F. *Chem. Rev.*, **2011**, *111*, 5434. (h) Yang, G. P.; Hou, L.; Luan, X. J.; Wu, B. A.; Wang, Y. Y. *Chem. Soc. Rev.*, **2012**, *41*, 6992. (i) Tian, D. Q.; Li, Chen, Y.; Zhang, Y. H.; Chang, Z.; Bu, X. H. *Angew. Chem., Int. Ed.*, **2014**, *53*, 837.

(2) (a) Kitaura, R.; Seki, K.; Akiyama, G.; Kitagawa, S. *Angew. Chem., Int. Ed.*, **2003**, *42*, 428. (b) Matsuda, R.; Kitaura, R.; Kitagawa, S.; Kubota, Y.; Belosludov, R. V.; Kobayashi, T. C.; Sakamoto, H.; Chiba, T.; Takata, M.; Kawazoe, Y.; Mita, Y. *Nature*, **2005**, *436*, 238. (c) Ockwig, N. W.; Delgado-Friederichs, O.; O'Keeffe, M.; Yaghi, O. M.; *Acc. Chem. Res.*, **2005**, *38*, 176. (d) Yaghi, O. M. *Nat. Mater.*, **2007**, *6*, 92. (e) Chen, X. D.; Zhao, X. H.; Chen, M.; Du, M. *Chem.-Eur. J.* **2009**, *15*, 12974. (f) Li, S.; Luo, J.; Sun, Z.; Zhang, S.; Li, L.; Shi, X.; Hong, M. *Cryst. Growth Des.*, **2013**, *13*, 2675; (g) Liao, P. Q.; Zhou, D. D.; Zhu, A. X.; Jiang, L.; Lin, R. B.; Zhang, J. P.; Chen, X. M. *J. Am. Chem. Soc.*, **2012**, *134*, 17380; (h) Zhang, M. D.; Di, C. M.; Qin, L.; Yang, Q. X.; Li, Y. Z. Guo, Z. J.; Zheng, H. G. *CrystEngComm*, **2013**, *15*, 227.

(3) (a) Batten, S. R.; Robson, R. *Angew. Chem., Int. Ed.*, **1998**, *37*, 1460. (b) Batten, S. R. *CrystEngComm*, **2001**, *3*, 67. (c) Blatov, V. A.; Carlucci, L.; Ciani, G.; Proserpio, D. M. *CrystEngComm*, **2004**, *6*, 377. (d) Carlucci, L.; Ciani, G.; Proserpio, D. M. *Coord. Chem. Rev.*, **2003**, *246*, 247. (e) Baburin, I. A.; Blatov, V. A.; Carlucci, L.; Ciani, G.; Proserpio, D. M. *Cryst. Growth Des.*, **2008**, *8*, 519. (f) Baburin, I. A.; Blatov, V. A.; Carlucci, L.; Ciani, G.; Proserpio, D. M. *CrystEngComm*, **2008**, *10*, 1822. (g) Baburin, I. A.; Blatov, V. A.; Carlucci, L.; Ciani, G.; Proserpio, D. M. *J. Solid State Chem.*, **2005**, *178*, 2452.

(4) (a) Shin, D. M.; Lee, I. S.; Chung, Y. K.; Lah, M. S. *Chem. Commun.*, **2003**, 1036. (b) Wu, H.; Yang, J.; Su, Z. M.; Batten, S. R.; Ma, J. F. *J. Am. Chem. Soc.* **2011**, *133*, 11406. (c) Wang, C. C.; Chung, W. C.; Lin, H. W.; Dai, S. C.; Shiu, J. S.; Lee, G. H.; Sheu, H. S.; Lee, W. *CrystEngComm*, **2011**, *13*, 2130. (d) Liu, B.; Yang, J.; Yang, G. C.; Ma, J. F. *Inorg. Chem.* **2013**, *52*, 84. (e) Hu, F. L.; Wu, W.; Liang, P.; Gu, Y. Q.; Zhu, L. G.; Wei, H.; Lang, J. P. *Cryst. Growth Des.* **2013**, *13*, 5050. (f) Liu, B.; Li, D. S.; Hou, L.; Yang, G. P.; Wang, Y. Y.; Shi, Q. Z. *Dalton Trans.* **2013**, *42*, 9822.

(5) (a) Qin, C.; Wang, X. L.; Carlucci, L.; Tong, M. L.; Wang, E. B.; Hu, C. W.; Xu, L. *Chem. Commun.* **2004**, *47*, 1876. (b) Wang, X. L.; Qin, C.; Wang, E. B.; Li, Y. G.; Su, Z. M.; Xu, L.; Carlucci, L. *Angew. Chem., Int. Ed.* **2005**, *44*, 5824. (c) Zheng, B.; Bai, J. F. *CrystEngComm*, **2009**, *11*, 271. (d) Li, L. J.; Qin, C.; Wang, X. L.; Wang, S.; Zhao, L.; Yang, G. S.; Wang, H. N.; Yuan, G.; Shao, K. Z.; Su, Z. M. *CrystEngComm*, **2012**, *14*, 124. (e) Chen, H. Y.; Xiao, D. R.; Yang, J.; Yan, S. W.; He, J. H.; Wang, X.; Ye, Z. L.; Wang, E. B. *Inorg. Chem. Commun.* **2012**, *20*, 157.

(6) (a) Tong, M. L.; Chen, X. M.; Batten, S. R. *J. Am. Chem. Soc.*, **2003**, *125*, 16170. (b) Wang, X. L.; Qin, C.; Wang, E. B.; Su, Z. M. *Chem.–Eur. J.*, **2006**, *12*, 2680. (c) Kathalikkattil, A. C.; Bisht, K. K.; Aliaga-Alcalde, N.; Suresh, E. *Cryst. Growth Des.*, **2011**, *11*, 1631. (d) Wang, C. Y.; Wilseck, Z. M.; LaDuca, R. L. *Inorg. Chem.*, **2011**, *50*, 8997. (e) Zhai, Q. G.; Niu, J. P.; Li, S. N.; Jiang, Y. C.; Hu, M. C.; Batten, S. R. *CrystEngComm* **2011**, *13*, 4508.

(7) (a) Cao, X. Y.; Zhang, J.; Li, Z. J.; Cheng, J. K.; Yao, Y. G. *CrystEngComm*, **2007**, 9, 806. (b) Huang, X. H.; Sheng, T. L.; Xiang, S. C.; Fu, R. B.; Hu, S. M.; Li, Y. M.; Wu, X. T. *Inorg. Chem.*, **2007**, *46*, 497. (c) Chen, H. Y.; Xiao, D. R.; He, J. H.; Li, Z. F.; Zhang, G. J.; Sun, D. Z.; Yuan, R.; Wang, E. B.; Luo, Q. L. *CrystEngComm*, **2011**, *13*, 4988.

(8) (a) Maji, T. K.; Matsuda, R.; Kitagawa, S. *Nat. Mater.*, **2007**, *6*, 142. (b) LaDuca, R. L. *Coord. Chem. Rev.*, **2009**, *253*, 1759. (c) Ma, L. F.; Wang, L. Y.; Du, M.; Batten, S. R. Inorg. Chem. 2010, 49, 365. (d) Alexandrov, E. V.; Blatov, V. A.; Kochetkov, A. V.; Proserpio, D. M. *CrystEngComm*, **2011**, *13*, 3947. (e) Béziau, A.; Baudron, S. A.; Pogozhev, D.; Fluck, A.; Hosseini, M. W. *Chem. Commun.*, **2012**, *48*, 10313. (f) Liao, Y. H.; Hsu, W.; Yang, C. C.; Wu, C. Y.; Chen, J. D.; Wang, J. C. *CrystEngComm*, **2013**, *15*, 3974. (g) Shen, J. J.; Li, M. X.; Wang, Z. X.; Duan, C. Y.; Zhu, S. R.; He, X. *Cryst. Growth Des.*, **2014**, *14*, 2818.

(9) (a) Yang, J.; Ma, J. F.; Batten, S. R.; Su, Z. M. *Chem. Commun.*, **2008**, 2233. (b) Li, Z. X.; Xu, Y.; Zuo, Y.; Li, L.; Pan, Q. H.; Hu, T. L.; Bu, X. H. *Cryst. Growth Des.* **2009**, *9*, 3904. (c) Ahmad, M.; Das, R.; Lama, P.; Poddar, P.; Bharadwaj, P. K. *Cryst. Growth Des.*, **2012**, *12*, 4624. (d) Sengupta, S.; Ganguly, S.; Goswami, A.; Bala, S.; Bhattacharya, S.; Mondal, R. *CrystEngComm*, **2012**, *14*, 7428. (e) Yi, F. Y.; Yang, W.; Sun, Z. M. *J. Mater. Chem.*, **2012**, *22*, 23201. (f) Zhang, Z.; Ma, J. F.; Liu, Y. Y.; Kan, W. Q.; Yang, J. *CrystEngComm*, **2013**, *15*, 2009. (g) Liu, J.; Zhang, H. B.; Tan, Y. X.; Wang, F.; Kang, Y.; Zhang, J. *Inorg. Chem.* **2014**, *53*, 1500-1506.

(10) Yang, J. X.; Qin, Y. Y.; Cheng, J. K.; Yao, Y. G. *Cryst. Growth Des.* **2014**, 14, 1047-1056.

(11) (a) Carlucci, L.; Ciani, G.; Proserpio, D. M.; Rizzato, S. *CrystEngComm*, **2002**, *4*, 121. (b) Zheng, Y. Q.; Zhang, J.; Liu, J. Y. *CrystEngComm*, **2010**, *12*, 2740. (c) Li, B. Y.; Li, G. H.; Liu, D.; Peng, Y.; Zhou, X. J.; Hua, J.; Shi, Z.; Feng, S. H. *CrystEngComm*, **2011**, *13*, 1291. (d) Wang, J. J.; Hu, T. L.; Bu, X. H. *CrystEngComm*, **2011**, *13*, 5152.

(12) Sheldrick, G. M. *SADABS, Program for Area Detector Adsorption Correction*, Institute for Inorganic Chemistry, University of Göttingen: Göttingen, Germany, **1996**.

(13) Sheldrick, G. M. *SHELXL-97, Program for Solution of Crystal Structures*, Institute for Inorganic Chemistry, University of Göttingen: Göttingen, Germany, **1997**.

(14) Yang, J. X.; Qin, Y. Y.; Cheng, J. K.; Yao, Y. G. *Cryst. Growth Des.* **2014**, 14, 1047.

(15) (a) Xiao, D. R.; Li, Y. G.; Wang, E. B.; Fan, L. L.; An, H. Y.; Su, Z. M.; Xu, L. *Inorg. Chem.* **2007**, *46*, 4158. (b) Zhang, L. P.; Yang, J.; Ma, J. F.; Jia, Z. F.; Xie, Y. P.; Wei, G. H. *CrystEngComm* **2008**, *10*, 1410. (c) Liu, G. X.; Zhu, K.; Xu, H. M.; Nishihara, S.; Huang, R.

Y.; Ren, X. M. *CrystEngComm* **2009**, *11*, 2784. (d) Li, B. Y.; Zhang, Y. M.; Li, G. H.; Liu, D.; Chen, Y.; Hu, W. W.; Shi, Z.; Feng, S. H. *CrystEngComm* **2011**, *13*, 2457.

(16) (a) Chen, P. K.; Qi, Y.; Che, Y. X.; Zheng, J. M. *CrystEngComm* **2010**, *12*, 720. (b) Farnum, G. A.; LaDuca, R. L. *Cryst. Growth Des.* **2010**, *10*, 1897. (c) Sun, L. X.; Qi, Y.; Wang, Y. M.; Che, Y. X.; Zheng, J. M. *CrystEngComm* **2010**, *12*, 1540. (d) Liu, Y. Y.; Wang, Z. H.; Yang, J.; Liu, B.; Liu Y. Y.; Ma, J. F. *CrystEngComm* **2011**, *13*, 3811. (e) Gao, J. Z.; Yang, J.; Liu, Y. Y.; Ma, J. F. *CrystEngComm* **2012**, *14*, 8173. (f) Liu, Y. Y.; Liu, H. Y.; Ma, J. F.; Yang, Y.; Yang, J. *CrystEngComm* **2013**, *15*, 1897.

(17) (a) O' Keeffe, M.; Peskov, M. A.; Ramsden, S. J.; Yaghi, O. M. *Acc. Chem. Res.* **2008**, *41*, 1782. database available at http://rcsr.anu.edu.au/. (b) O' Keeffe, M.; Yaghi, O. M. *Chem. Rev.* **2012**, *112*, 675. (c) O' Keeffe, M.; Yaghi, O. M. *Chem. Rev.* **2014**, *114*, 1343. (d) Ramsden, S. J.; Robins, V.; Hyde, S. T. *Acta Crystallogr.* **2009**, *A65*, 81 database available at http://epinet.anu.edu.au.

(18) (a) Carlucci, L.; Ciani, G.; Moret, M.; Proserpio, D.M.; Rizzato, S. *Angew. Chem. Int. Ed.*, **2000**, *39*, 1506. (b) Xiao, D. R.; Li, Y. G.;

Wang, E. B., Fan, L. L.; An, H. Y.; Su, Z. M., Xu,L. *Inorg. Chem.*, **2007**, *46*, 4158. (c) He, J. H.; Xiao, D. R.; Chen, H. Y.; Yan, S. W.; Sun, D. Z.; Wang, X.; Yang, J.; Yuan, R.; Wang, E. B. *Inorg. Chim. Acta*, **2012**, *385*, 170.

(19) (a) Chang, Z.; Zhang, A. S.; Hu, T. L.; Bu, X. H. *Cryst. Growth Des.* **2009**, *9*, 4840. (b) Wu, H.; Liu, H. Y.; Liu, Y. Y.; Yang, J.; Liu, B.; Ma, J. F. *Chem. Commun.* **2011**, *47*, 1818. (c) Guo, F.; Wang, F.; Yang, X. L.; Zhang, J. *Inorg. Chem.* **2012**, *51*, 9677.

**Table 1** Crystal data and structure refinements for compound **1-6**.

| Compound | 1 | 2 | 3 | 4 | 5 | 6 |
|---|---|---|---|---|---|---|
| Empirical formula | $C_{17}H_{20}CdN_2O_6$ | $C_{30}H_{40}CdN_4O_9$ | $C_{32}H_{50}Cd_2N_5O_{17}$ | $C_{60}H_{70}Cd_2N_8O_{11}$ | $C_{49}H_{74}Cd_2N_6O_{18}$ | $C_{38}H_{48}Cd_2N_4O_{10}$ |
| Formula eight | 460.74 | 712.99 | 1001.49 | 1304.01 | 1259.8 | 945.62 |
| crystal system | Monoclinic | Triclinic | Monoclinic | Monoclinic | Orthorhombic | Monoclinic |
| space group | $P 2_1/c$ | $P\bar{1}$ | $P 2_1/n$ | $C 2/c$ | $C 222_1$ | $P 2/c$ |
| $a$ (Å) | 8.197(2) | 9.3510(5) | 13.4668(4) | 21.9308(10) | 20.6271(8) | 15.2083(5) |
| $b$ (Å) | 18.032(5) | 12.0189(7) | 14.3053(3) | 11.2167(4) | 13.6669(6) | 9.1886(3) |
| $c$ (Å) | 12.981(4) | 16.2548(6) | 21.8218(5) | 24.9201(11) | 20.6839(9) | 27.5808(8) |
| $\alpha$ (deg) | 90 | 78.851(4) | 90 | 90 | 90 | 90 |
| $\beta$ (deg) | 104.558(5) | 84.234(4) | 93.302(2) | 97.612(4) | 90 | 93.940(3) |
| $\gamma$ (deg) | 90 | 74.569(5) | 90 | 90 | 90 | 90 |
| $V$ (Å$^3$) | 1857.1(10) | 1725.45(15) | 4196.92(18) | 6076.1 | 5831.0(4) | 3845.1(2) |
| $Z$ | 4 | 2 | 4 | 4 | 4 | 4 |
| $D_{calcd}$ (mg m$^{-3}$) | 1.648 | 1.353 | 1.566 | 1.419 | 1.412 | 1.633 |
| $F$ (000) | 920.0 | 716.0 | 1988.0 | 2656.0 | 2520.0 | 1728 |
| Reflcn collcd/ unique | 14529/4236 | 13062/6078 | 16188 / 7371 | 12696 / 5354 | 7363 / 4492 | 15224 / 6763 |
| GOF on $F^2$ | 1.087 | 1.052 | 1.007 | 1.046 | 0.917 | 1.018 |
| $R_1$, $wR_2$ [$I > 2\sigma(I)$]$^a$ | 0.0351, 0.0914 | 0.0704, 0.1982 | 0.0591, 0.1731 | 0.0740, 0.2194 | 0.0393, 0.1008 | 0.0309, 0.0671 |
| $R_1$, $wR_2$ (all data)$^b$ | 0.0424, 0.0954 | 0.0818, 0.2122 | 0.0761, 0.1888 | 0.0904, 0.2390 | 0.0495, 0.1107 | 0.0460, 0.0747 |

$^a R_1 = \sum||F_o|-|F_c||/\sum|F_o|$, $^b wR_2 = [\sum w(F_o^2 - F_c^2)^2/\sum w(F_o^2)^2]^{1/2}$



{[Cd(fum)(bpp)(H_2O)]·(H_2O)}_n  (1)

{[Cd(fum)(bpp)_2]·(H_2O)_5}_n  (2)

{[Cd_2(suc)_{1.5}(bpp)_2(NO_3)(H_2O)_2]·6H_2O}_n  (3)

{[Cd(suc)(bpp)_2]·(H_2O)_{1.5}}_n  (4)

{[Cd_2(glu)_2(bpp)_3]·10H_2O}_n  (5)

{Cd(adp)(bpp)(H_2O)}_n  (6)
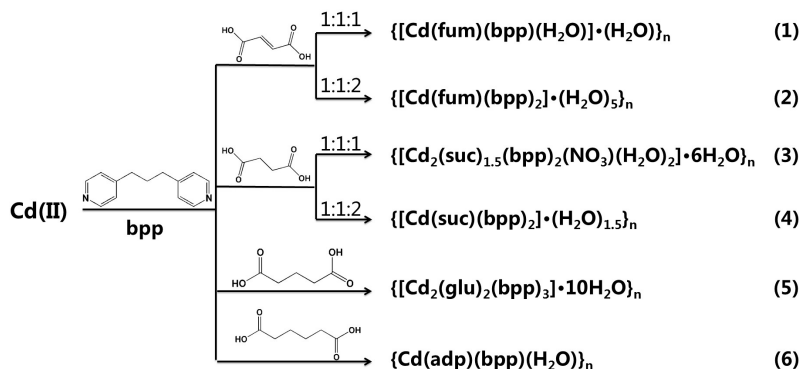
**Scheme 1** Stoichiometric and secondary ligand control in the synthesis of compounds **1–6**.
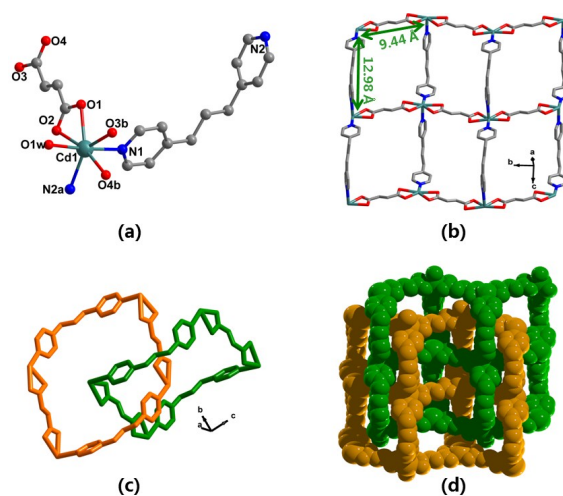


**Figure 1.** (a) View of asymmetric unit for **1** (symmetry codes: a = $x$, $y$, 1+$z$; b = −2−$x$, 0.5+$y$, 0.5−$z$.) (b) View of the $4^4$-**sql** sheet in the structure of **1**. (c) View of the 4-crossing [2]-catenane. (d) Space-filling diagram of the two-fold parallel interpenetration of the 2D layers in **1**
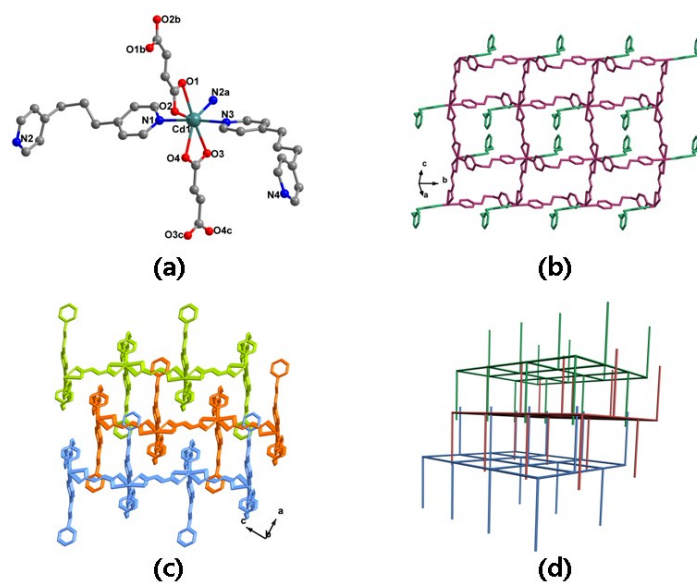


**Figure 2.** (a) View of the coordinated environment of Cd(II) centers in compound **2** (symmetry codes: a= $x$, 1+$y$, $z$; b= 2–$x$, 1–$y$, –$z$; c= 1–$x$, 1–$y$, 1–$z$). Lattice water molecules and hydrogen atoms have been omitted for clarity; (b) A single 2D square ($4^4$) motif showing the dangling arms; (c) Perspective and (d) schematic views of the 2D→3D polypseudo-threading network.
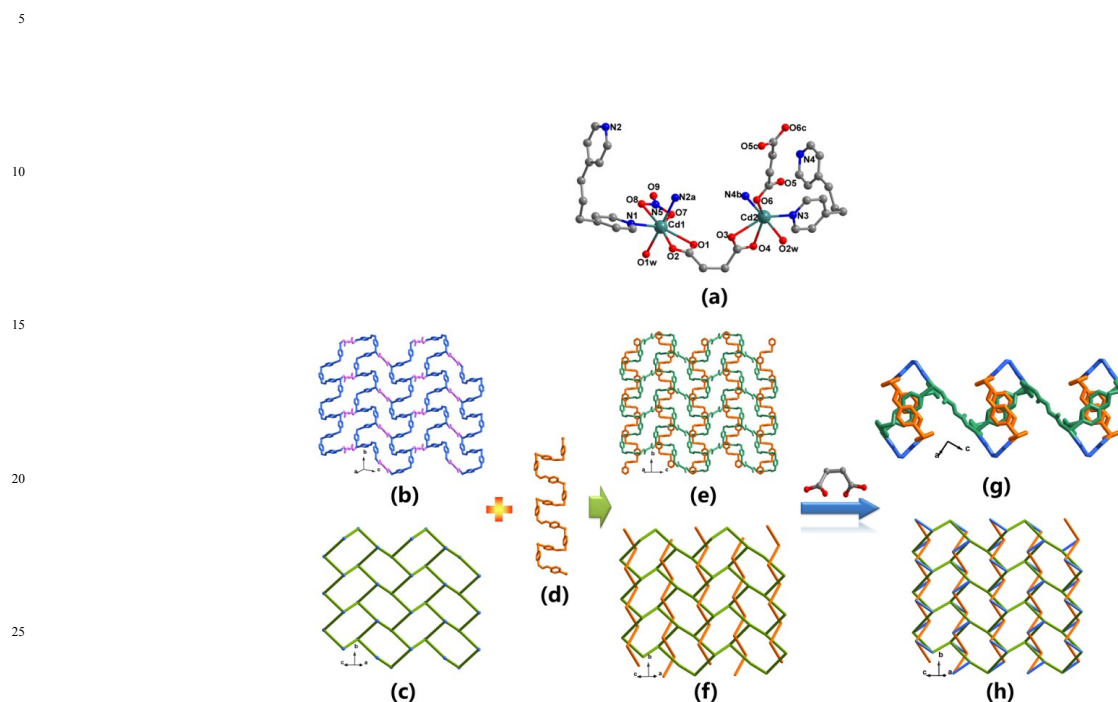
**Figure 3.** (a) View of coordination environment of the Cd(II) ions in compound **3**. (The hydrogen atoms have been omitted for clarity)(Symmetry code: a = 0.5−*x*, −0.5+*y*, 0.5−*z*; b = 0.5−*x*, 0.5+*y*, 0.5−*z*; c = −*x*, −*y*, 1−*z*). The perspective (b) and schematic (c) view of the 2D undulated (6, 3) network in **3**. (d) The 1D zigzag chain formed by Cd1 atoms and bpp-A ligands. The perspective (e) and schematic (f) view of 1D zigzag chains (orange) threading into a 2D (6, 3) sheet (green). (g) The 2D sheet and 1D chains are further interconnected by suc-C (blue) resulting in a self-penetrating framework. (h) The (3, 4)-connected self-penetrating 2D net of **3**.
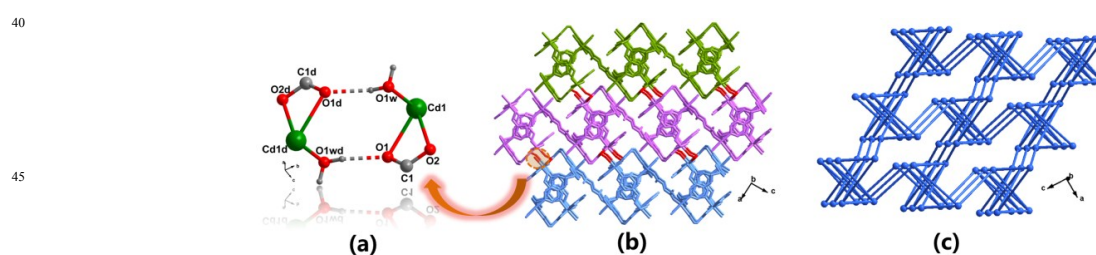


**Figure 4.** (a) View of the hydrogen bonding interactions among the coordinated water molecules and carboxylate anions. (Symmetry codes: d = −*x*,−*y*, −*z*) (Dotted lines represent H-bonds). (b) View of the 3D supramolecular structure connected by hydrogen-bonding interactions. (c) Schematic view of the **sxa** framework.

**(a)**



**(b)**



**(c)**



**(d)**



**(e)**
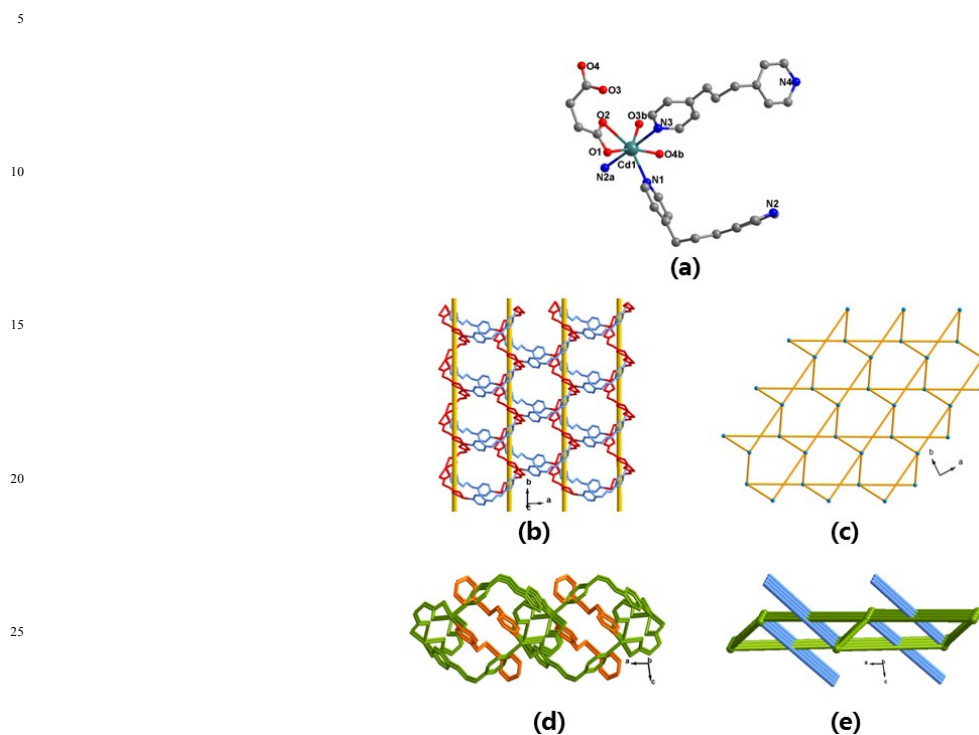
**Figure 5.** (a) Coordination environment of the Cd(II) cation in **4**. The hydrogen atoms are omitted for clarity. (Symmetry codes: a= 0.5+*x*, 0.5+*y*, *z*; b= 0.5−*x*, 0.5+*y*, −0.5−*z*). (b) The left- and right-handed helical [Cd(suc)] chains are linked by bpp ligands to form a 2D sheet. (c) 2D layer structure with {$4^2 \cdot 6^3 \cdot 8$} topology. (d) Perspective and (e) schematic views of the 2D self-threading structure in **4**.



**(a)**



**(b)**

glu-A

**(d)**

**(c)**

**(e)**

glu-B

**(f)**

**(g)**

**(h)**
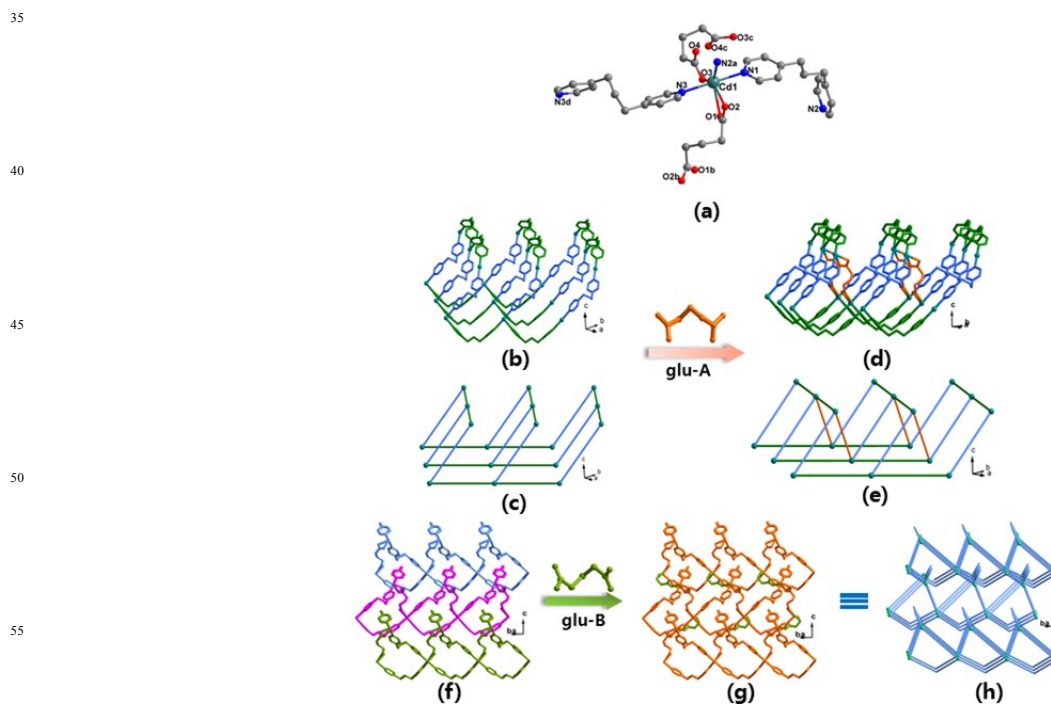
**Figure 6.** (a) The coordination environment of Cd(II) ion in **5** (symmetry code: a= 0.5+$x$, 0.5+$y$, $z$; b= $x$, −3−$y$, −$z$; c= −1−$x$, $y$, −0.5−$z$; d= $x$, −2−$y$, −$z$). The perspective (b) and schematic (c) view of the 2D T-shaped bilayer in **5**. The perspective (d) and schematic (e) view of 2D T-shaped bilayer reinforced by glu-A (orange) ligands. (f) The perspective view of the 2D→3D interpenetration. (g) The 2D→3D interpenetrating structure further linked by glu-B (green) ligands resulting in a self-penetrating framework. (h) Schematic perspective of the self-penetrating 5-connected uninodal **htp** network of **5**.
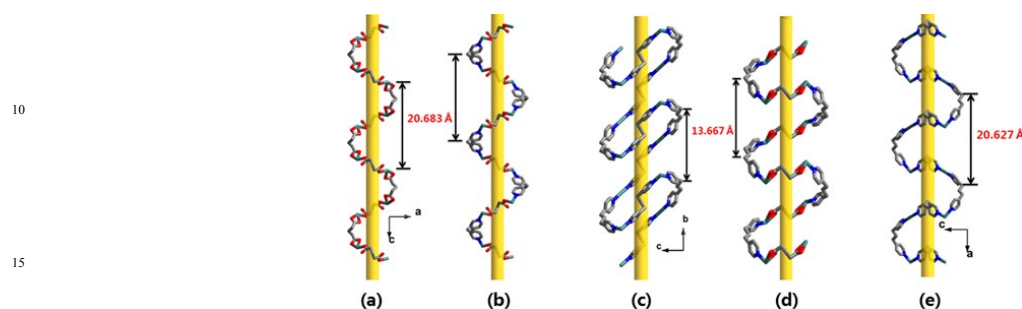


**Figure 7.** Views of the five types of helices in **5**: (a) the first, (b) the second, (c) the third, (d) the forth, and (e) fifth.
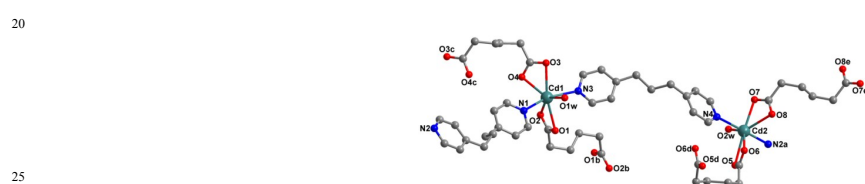


**Figure 8.** View of the coordinated environment of Cd(II) centers in compound **6** (symmetry codes: a= $x$, $y$, −1+$z$; b= −$x$, −$y$, −$z$; c= −$x$, $y$, 0.5−$z$; d= 1−$x$, $y$, −0.5−$z$; e= 1−$x$, 1−$y$, −1−$z$;). Hydrogen atoms have been omitted for clarity.
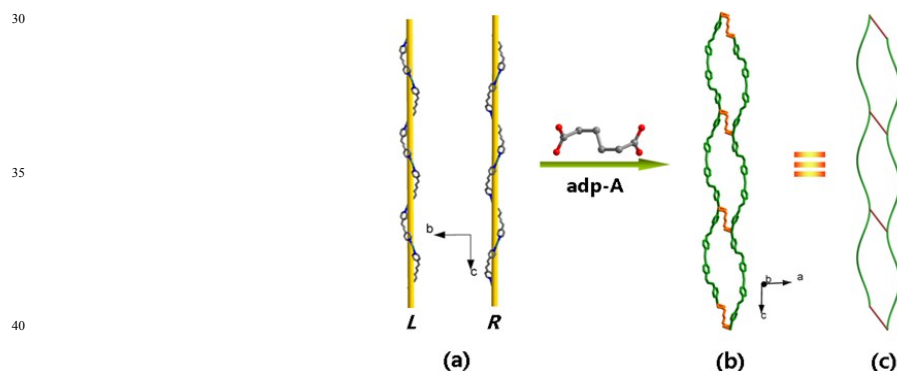


**Figure 9.** The left- and right-handed helical chains [Cd(bpp)]$_n$ (b) are associated together by the adp-A$^{2-}$ anions to build a 1D ladder.(c) Schematic representation of the 1D ladder.
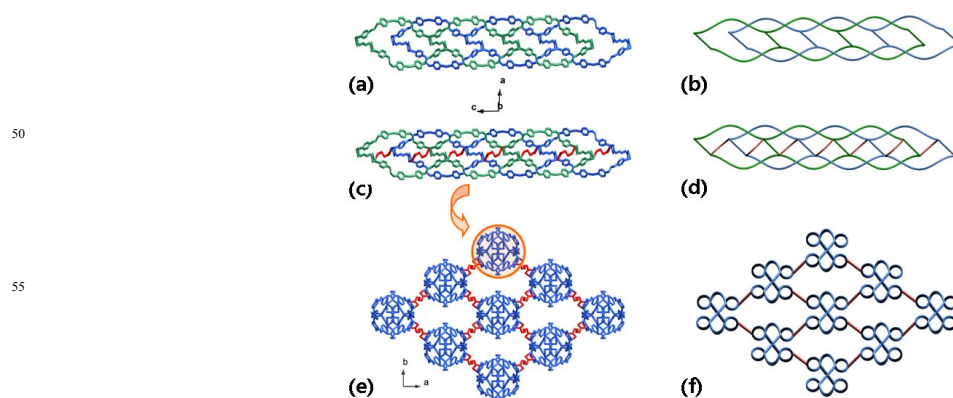
**Figure 10.** (a) Perspective and (b) schematic views of the 1D+1D→1D polycatenane entanglement of ladder pairs. (c) Perspective and (d) schematic views of the polycatenane entanglement further interconnected by adp-B resulting in a self-penetrating chain. (e) and (f) Representation of the 3D network composed of 1D self-penetrating chains and adp-D anions, viewed along the *c* axis.



(a)    (b)

(c)    (d)
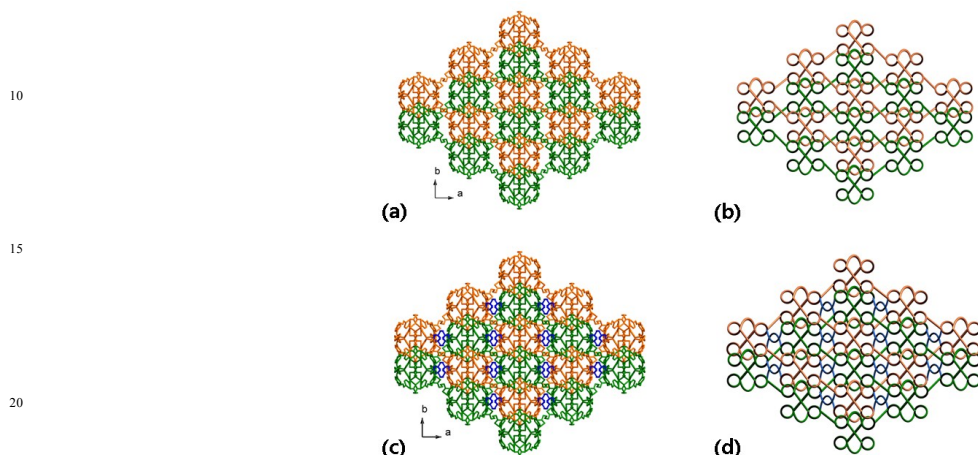
**Figure 11.** (a) Two independent 3D frameworks further interpenetrate each other. (b) Schematic representation of the two-fold interpenetration. (c) The uninodal 4-connected self-penetrating **sxa** network derived from the crosslinked two-fold interpenetrating (3,4)-connected 3D nets. (Blue lines represent adp-D ligands) (d) Schematic representation of the self-penetrating network.

**Table 2** Geometrical parameters of aliphatic dicarboxylate ligands and bpp ligands in the compounds **1−6**.

| Compound No. | aliphatic dicarboxylate ligands | | bpp ligands | |
|---|---|---|---|---|
| | spacer | separation between Cd atoms[a] (Å) | conformation of bpp ligands | Dihedral angles between the two pyridyl rings (°) |
| **1** | –CHCH– | 9.44 | *TT* | 82.11 |
| **2** | –CHCH– | 9.29, 9.31 | *TG, TT* | 86.16, 72.16 |
| **3** | –(CH₂)₂– | 7.05, 9.50 | *TG, TG* | 87.91, 79.79 |
| **4** | –(CH₂)₂– | 7.02 | *TG, TG* | 81.15, 55.35 |
| **5** | –(CH₂)₃– | 7.52, 8.58 | *TT, GG'* | 83.09, 24.76 |
| **6** | –(CH₂)₄– | 7.64, 7.52, 9.80, 10.54 | *TG, TT* | 15.69, 40.93 |
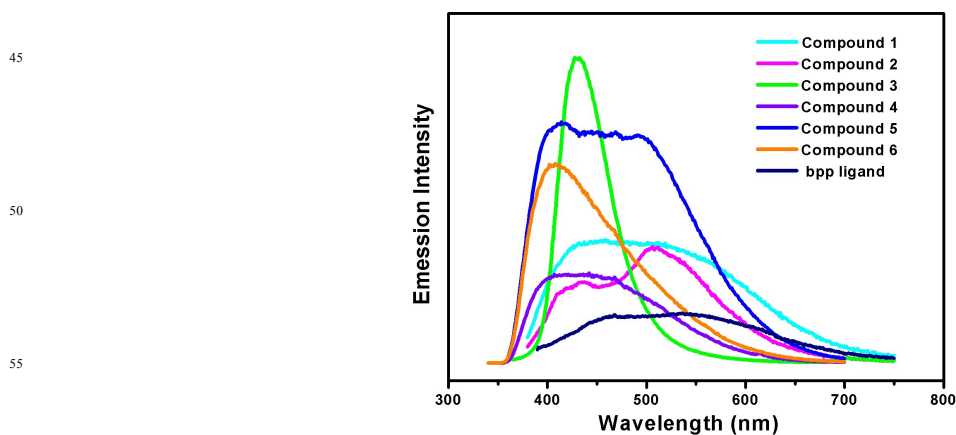
**Figue 12.** The fluorescent spectra of compounds **1-6** in the solid-state at room temperature.